



Since January 2020 Elsevier has created a COVID-19 resource centre with free information in English and Mandarin on the novel coronavirus COVID-19. The COVID-19 resource centre is hosted on Elsevier Connect, the company's public news and information website.

Elsevier hereby grants permission to make all its COVID-19-related research that is available on the COVID-19 resource centre - including this research content - immediately available in PubMed Central and other publicly funded repositories, such as the WHO COVID database with rights for unrestricted research re-use and analyses in any form or by any means with acknowledgement of the original source. These permissions are granted for free by Elsevier for as long as the COVID-19 resource centre remains active.



Cis-acting structural element in 5' UTR is essential for infectivity of porcine reproductive and respiratory syndrome virus

Fei Gao^{a,b}, Jiaqi Lu^b, Huochun Yao^a, Zuzhang Wei^b, Qian Yang^{a,*}, Shishan Yuan^{b,**}

^a College of Veterinary Medicine, Nanjing Agricultural University, Nanjing, Jiangsu Province 210095, PR China

^b Department of Swine Infectious Diseases, Shanghai Veterinary Research Institute, Chinese Academy of Agricultural Sciences, Shanghai 200241, PR China

ARTICLE INFO

Article history:

Received 16 March 2011

Received in revised form 30 August 2011

Accepted 31 August 2011

Available online 7 September 2011

Keywords:

PRRSV

5' UTR

Cis-acting elements

Stem-loop structures

Virus replication

ABSTRACT

It is believed that the genomic 5' untranslated region (UTR) of Arterivirus plays crucial roles in viral genomic replication, subgenomic mRNA transcription and protein translation, yet the structure and function still remain largely unknown. In this study, we conducted serial nucleotide truncation, ranging from 1 to 190 nucleotides, to the 5' UTR of the porcine reproductive and respiratory syndrome virus (PRRSV) infectious full-length cDNA clone pAPRRS. In vitro synthetic RNAs were transfected into MARC-145 cells for further genetic and virologic analysis. Our results demonstrated that the first three nucleotides of PRRSV 5' UTR were dispensable for virus viability, which however was repaired with foreign sequences. In order to assess if the primary sequence or structural element play more important regulatory roles, the CMV promoter-driven 5' UTR truncation mutant cDNA clones were directly transfected into the BHK-21 cell lines. We found that PRRSV tolerated the first 16 nucleotides sequence alteration of 5' UTR without losing virus viability. However, these revertant viruses contained a range of non-templated with unknown origin exogenous nucleotides in the repaired 5' end. Further analyses revealed that the 5' proximal stem-loop 1 (SL1) in the highly structured 5' UTR was invariably required for virus infectivity. Taken together, we conclude that authentic 5'-proximal primary sequence is nonessential, but the resultant structural elements are probably indispensable for PRRSV infectivity.

© 2011 Elsevier B.V. All rights reserved.

1. Introduction

Nidoviruses have quite distinctive replication and transcription processes compared with other single-stranded, plus-strand RNA viruses and feature the most complex genomic organization (Pasternak et al., 2006; Snijder and Meulenberg, 1998). There are four family members in the order Nidovirales, which includes coronavirus, torovirus, arterivirus and ronivirus (Pasternak et al., 2006). Nidoviruses cause a variety of infectious diseases, for example, severe acute respiratory syndrome (SARS) virus in humans, which gripped the attention of the world in 2003, is the member of coronavirus (Drosten et al., 2003; Ksiazek et al., 2003; Peiris et al., 2003). There are also severe nidoviral diseases in animals, such as porcine reproductive and respiratory syndrome virus (PRRSV) (Cavanagh, 1997; Snijder, 2001), which is a member of the family Arteriviridae

together with equine arteritis virus (EAV), simian hemorrhagic fever virus (SHFV), and the lactate dehydrogenase-elevating virus of mice (LDV) (den Boon et al., 1991; Pasternak et al., 2006; Snijder and Meulenberg, 1998). Since 2006, massive outbreaks of highly pathogenic PRRSV have overwhelmed the swine industry in China and its neighboring countries (Lv et al., 2008; Tian et al., 2007; Zhou and Yang, 2010). Despite massive efforts have been directed towards prevention and control of PRRS, little improvement has been shown and the latter is still the biggest threat to the swine industry, particularly in developing countries. One of the reasons for such ineffective PRRS control is that many puzzles remain unearthed for PRRSV biology.

PRRSV genome has a 5' cap and a 3' poly (A) tail and is ~15 kb in length. There are at least nine open reading frames (ORFs), flanked by the 5' UTR, 3' UTR, respectively, which are believed to play pivotal regulatory roles in PRRSV life cycle (Sun et al., 2010, 2007; Verheije et al., 2001, 2002). Like other nidoviruses, PRRSV generates a 3' co-terminal nested set of subgenomic mRNA (sg mRNA) to produce structural proteins. PRRSV sg mRNAs also contain a common 5' leader sequence, which comes from the genomic 5' end (Pasternak et al., 2006; Snijder and Meulenberg, 1998). The sg mRNA synthesis involves a process of unique discontinuous RNA transcription similar with the RNA recombination (Pasternak et al., 2006; van Marle et al., 1999). During the process of discontinuous RNA transcription,

* Corresponding author at: College of Veterinary Medicine, Nanjing Agricultural University, 1 Weigang, Nanjing 210095, Jiangsu, China. Tel.: +86 25 84395817; fax: +86 25 84398669.

** Corresponding author at: Shanghai Veterinary Research Institute, Chinese Academy of Agricultural Sciences, No. 518, Ziyue Road, Minhang District, Shanghai 200241, China. Tel.: +86 21 34293773; fax: +86 21 54081818.

E-mail addresses: zxbyq@njau.edu.cn (Q. Yang), shishanyuan@hotmail.com (S. Yuan).

the transcription-regulating sequence (TRS) plays a crucial role by base-pairing interaction between body TRS (TRS-B) and Leader TRS (TRS-L) during the synthesis of minus-strand RNA (Pasternak et al., 2006, 2001; Sawicki and Sawicki, 1995). The TRS-Bs in the genome would act as attenuation signals for minus-strand RNA synthesis, after which the nascent minus strand, having an anti TRS-B at its 3' end, would be guided to the 5'-proximal region of the template, through a base-pairing interaction with the TRS-L. Following the addition of the anti-leader to the nascent minus strands, the sg-length minus strands would serve as templates for transcription. However, many molecular details for such a unique transcription process remain to be investigated. In particular, what are the roles of the TRS-flanking sequences and/or local or genomic global RNA structures? Does Arteriviral RNA synthesis also require cross-talk between the genomic termini, as described for other positive-strand RNA viruses (Filomatori et al., 2006; Suzuki et al., 2008)?

It is generally believed that RNA viruses require authentic genomic termini for RNA synthesis. Nonviral terminal sequences usually have deleterious effects on viral replication (Boyer and Haenni, 1994; Herold and Andino, 2000). Intriguingly, Choi et al. (2006) reported that PRRSV tolerated deletion of the 5'-proximal 7 nucleotides (¹AUGACGU⁷) without the loss of the viral infectivity. These authors found that the rescued PRRSVs contained a range of novel 5' AU-rich sequences without known origin (Choi et al., 2006). We hypothesized that the 5' UTR structural elements rather than the primary sequences were required for PRRSV replication.

In this study, reverse genetic study was conducted on a type II PRRSV infectious cDNA clone pAPRRS, which was dually controlled by both CMV promoter and T7 promoter (Yuan and Wei, 2008). The *in vitro* RNA transcripts from T7 promoter were utilized to investigate if presence of the authentic 5'-terminal nucleotide sequence was required, while *in vivo* RNA transcripts from CMV promoter were intended for sequence specificity and/or structural RNA signal studies. Serial truncations of the 5'-proximal end of pAPRRS were performed. In the RNA-launched reverse genetics system (RGS), we found that the first 3 nucleotides (¹AUG³) at the very beginning of PRRSV 5' UTR were dispensable for virus viability, yet the deleted nucleotides were repaired with different sequences. In the DNA-launch system, we demonstrated that the first 16 nucleotides, ¹AUGACGUAUAGGUGUU¹⁶, of PRRSV 5' UTR could be altered by a combination of deletion and substitution in the *in vivo* RNA transcripts. However, the altered sequences were repaired with a variable length and largely AU-rich exogenous sequences in the rescued viruses. Surprisingly, in all cases the reverted AU-rich sequences were found to restore the original stem-loop 1 (SL1) structure of the PRRSV 5' UTR. Moreover, the infectivity of the transfected DNAs were found to be directly related to the presence of the SL1, which was probably a key for the initiation of PRRSV process. We therefore concluded that the structural RNA elements rather than primary sequences of the 5'-terminus of the PRRSV 5' UTR played more important regulatory roles in virus replication process.

2. Materials and methods

2.1. Viruses and cells

MARC-145 cells (ATCC, Manassas, VA) were cultured in MEM (Invitrogen) with 10% fetal bovine serum (FBS, Gibco-BRL, Gaithersburg, MD, USA) and were maintained with 2% FBS at 37°C in a humidified 5% CO₂ atmosphere as described previously (Yuan and Wei, 2008). Baby hamster kidney (BHK-21, ATCC CCL10) cells were grown in EMEM (ATCC, Manassas, VA, USA) complement with 10% FBS. The parental PRRSV vAPRRS (GenBank accession number: GQ330474) was used in this study as WT control for compari-

son with mutant viruses in all experiments. The supernatant of the infected cells was harvested after 80% cytopathic effect (CPE) appeared, then the virus were stored at –80 °C as stocks for further use.

2.2. Construction of mutant clones with nucleotide deletions in their 5' ends via site-directed PCR-based mutagenesis

Full-length infectious PRRSV cDNA clone pAPRRS (Yuan and Wei, 2008), was used for constructing a series of mutant full-length cDNA clone with different size of 5' terminal sequences deleted. For the convenient manipulation, a shuttle plasmid pCBSA was constructed, which spanned the T7 promoter and Afl II restriction endonuclease digestion site (nt 1688). Mutant forward primers and SR2573 (complementary to nt 2548–2573) are listed in Table 1. PCR reaction consisted of 30 cycles of 95 °C denaturation (30 s), 65 °C annealing (30 s) followed by extension at 72 °C for 2 min. After gel-purified, restricted enzymatic mapping and nucleotide sequencing, the final mutant full-length plasmids were assembled. They were named as pAPRRSD1, D3, D4, D5, D6, pAPRRSM1, M2, M3, M4, M5, M6, M7, M8, M9, M10, M11, M12, M13, M14, M15, M16, M17, M18, M19, M21, M22, M23, M44, M68, M99, M190, in addition, pAPRRSMz3 and Mz6, as shown in Fig. 1. pAS was used as a non-replicative plasmid control (Lu et al., 2011).

2.3. Transfection and viruses rescue

The WT plasmid DNA and mutant plasmids pAPRRSD1, D3, D4, D5, D6 were purified using a QIAprep Spin Miniprep kit (QIAGEN, Hilden, Germany), and linearized with Xho I restriction enzyme which located immediately downstream of the poly (A) tail, followed by purified with QIAquick PCR purification kit (QIAGEN, Hilden, Germany). 1 µg of purified products were used as templates for *in vitro* RNA transcription by T7 promoter, with T7 mMES-SAGE mMachine (Ambion Inc., Austin, TX). After removal of the template from reaction mixture using DNase I, the synthetic RNAs were verified by 1.2% native RNA agarose gel electrophoretic, and stored at –80 °C until use (Yuan and Wei, 2008). MARC-145 cells in 6-well plate were grown to 80% confluence and transfected with 2 µL the *in vitro* transcripts with 2 µL of DMRIE-C reagent (Invitrogen, Carlsbad, CA) according to the instruction manual. When CPE developed 80%, the supernatants were harvested and stored at –80 °C, designated as passage 0 (P0). P0 viral supernatants were serially passaged through plaque purification for five times, named as P1–P5, for further experiments use.

All of the mutants and WT cDNA clones were isolated by QIAprep Spin Miniprep kit and further identified by spectrophotometer 0.8% AGE. 3 µg of each DNAs, 15 µL of Lipofectamine™ LTX and 3 µL Plus Reagent (Invitrogen) were transfected into the BHK-21 cells (70% confluence) directly according to the manufacturer's protocol. The cell supernatants were harvested at 24 hpt, aliquoted and stored at –80 °C, as P0. P0 viral supernatants were used for passage by plaque purification in MARC-145 cells in 6-well plates as virus stocks (five passages, P1–P5) for use in further experiments as described previously (Yu et al., 2009).

2.4. Indirect immunofluorescence assay (IFA)

70% confluence of BHK-21 cells was grown in 12-well plate, and each well was transfected by WT, mutant clones and mock control for verifying viral nucleocapsid protein expression as previously report (Sun et al., 2010). The cell monolayer at 24 hpt was fixed with ice-cold methanol for 10 min at room temperature and then blocked with 0.1% bovine serum albumin (BSA) for 30 min, followed by incubation with monoclonal antibody against N protein of type II PRRSV (kindly provided by Dr. Ying Fang at South Dakota State Uni-

Table 1
Oligonucleotides used for RT-PCR mutagenesis and Northern blot analysis.

Name ^a	Sequence	Position	Application
SFTLM1	5'- <i>acatgcatgct</i> taatac <i>gactcactatagg</i> TGACGTATAGGTGTGGCTC-3'	2–21	PCR mutagenesis
SFTLM3	5'- <i>acatgcatgct</i> taatac <i>gactcactatagg</i> ACGTATAGGTGTGGCTCT-3'	4–22	PCR mutagenesis
SFTLM4	5'- <i>acatgcatgct</i> taatac <i>gactcactatagg</i> CGTATAGGTGTGGCTCTA-3'	5–23	PCR mutagenesis
SFTLM6	5'- <i>acatgcatgct</i> taatac <i>gactcactatagg</i> TATAGGTGTGGCTCTATG-3'	7–25	PCR mutagenesis
SFTLM8	5'- <i>acatgcatgct</i> taatac <i>gactcactatagg</i> TAGGTGTGGCTCTATGCC-3'	9–27	PCR mutagenesis
SFTLM10	5'- <i>acatgcatgct</i> taatac <i>gactcactatagg</i> GGTGTGGCTCTATGCCTT-3'	11–29	PCR mutagenesis
SFTLM12	5'- <i>acatgcatgct</i> taatac <i>gactcactatagg</i> TGTGGCTCTATGCCTTGA-3'	13–31	PCR mutagenesis
SFTLM14	5'- <i>acatgcatgct</i> taatac <i>gactcactatagg</i> ITGGCTCTATGCCTTGACA-3'	15–33	PCR mutagenesis
SFTLM16	5'- <i>acatgcatgct</i> taatac <i>gactcactatagg</i> GGCTCTATGCCTTGACATT-3'	17–35	PCR mutagenesis
SFTLM19	5'- <i>acatgcatgct</i> taatac <i>gactcactatagg</i> ICTATGCCTTGACATTGT-3'	20–38	PCR mutagenesis
SFTLM21	5'- <i>acatgcatgct</i> taatac <i>gactcactatagg</i> TATGCCTTGACATTGTAT-3'	22–40	PCR mutagenesis
SFTLM44	5'- <i>acatgcatgct</i> taatac <i>gactcactatagg</i> AGGAGCTGTGATCATTGA-3'	45–62	PCR mutagenesis
SFTLM68	5'- <i>acatgcatgct</i> taatac <i>gactcactatagg</i> CCAAAGCTTGCTGCACAG-3'	69–86	PCR mutagenesis
SFTLM190	5'- <i>acatgcatgct</i> taatac <i>gactcactatagg</i> ATGCTCTGGGATACTTGA-3'	191–207	PCR mutagenesis
SR343	5'- TAGCCCAACAGGTATCCTTCTC-3'	322–343	Nucleotide sequencing
SR683	5'- GGAGCGGCAGGTTGGTTAACACGTGA-3'	658–683	5' RACE
SR1124	5'- CTTCAGCCTCCGCTGATAGTACTTGC-3'	1098–1124	5' RACE
SR2573	5'- CTGCCAGGCCATCATGTCCGAAGTC-3'	2548–2573	PCR mutagenesis
Qc	5'- CCAGTGAGCAGAGTGACGAGGACTCGAGCTCAAGC(C) ₁₇ -3'		5' RACE
Qo	5'- CCAGTGAGCAGAGTGACG-3'		5' RACE
Qi	5'- GAGGACTCGAGCTCAAGC-3'		5' RACE
PR3	5'- AATTCGCGCCGATGGTTTCGCCAATTAATCTTACCCACACGGTCGC-3'	15,470–15,520	Probe for Northern Blot

^a Primer names are organized in groups. Prefixes: SF, forward PCR primer; SR, reverse PCR primer. The T7 promoter in bold located in front of the viral sequence, and the restriction endonuclease sites *Sph*I was indicated in italic letters underline. The number of nucleotide position in the primer name denoted the position in full-length PRRSV sequence GQ330474.

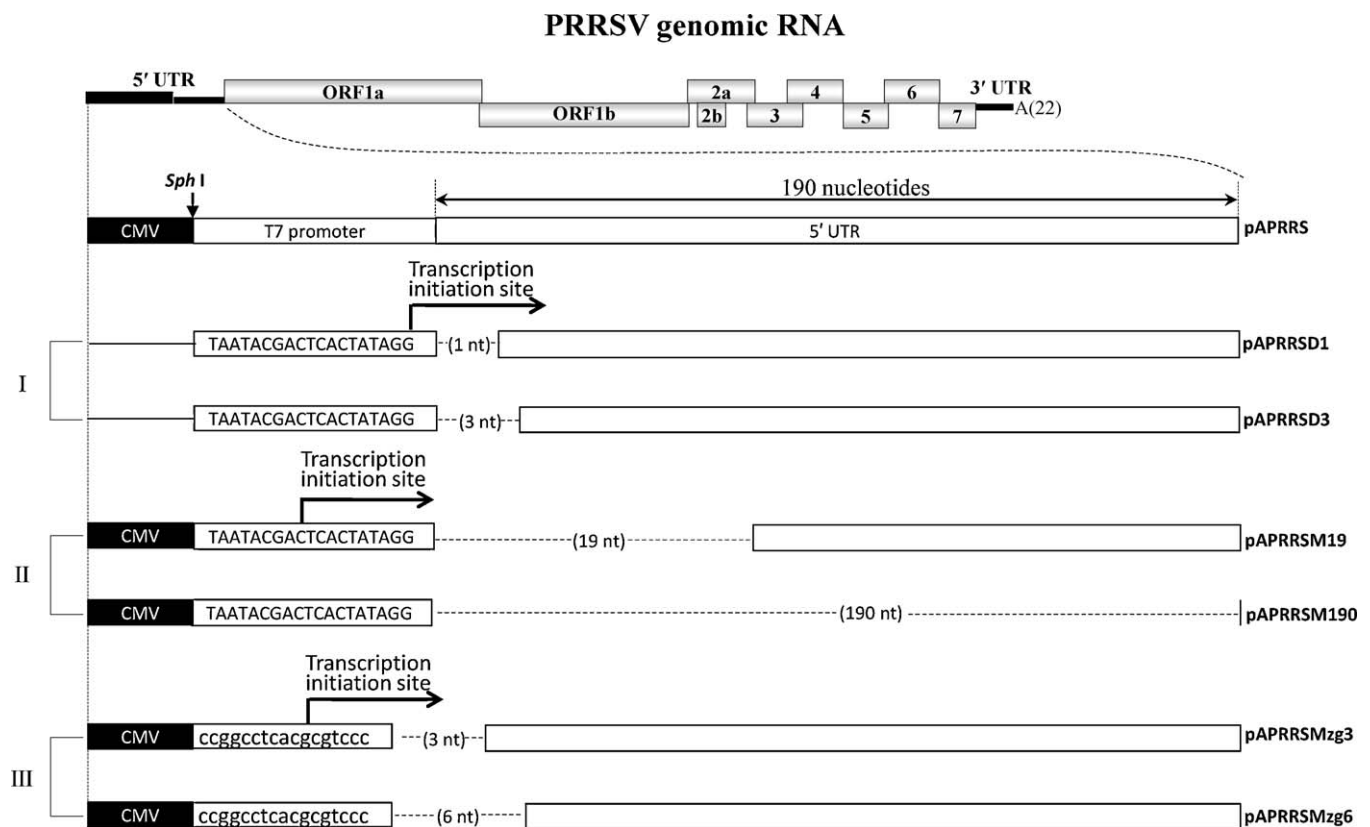


Fig. 1. Schematic representation of serial deletions of the PRRSV 5' UTR. The upper panel showed the PRRSV genomic organization, which had 9 encoding ORFs denoted by gray box, flanked by 5', 3' UTR and poly (A) tail. Group I represented pAPRRSD1 and SD3, which were used as T7 promoter-driven RNA-launched mutant analysis. Group II represented the CMV promoter-driven DNA-launched serial deletion mutants designated as pAPRRSM_x, x denoted the number of nucleotides (also in hyphen) deleted, using pAPRRSM19 and SM190 as representative. Group III represented pAPRRSMz₃ and Mz₆. White boxes indicated the authentic PRRSV sequence of 5' UTR. Hyphens showed deleted nucleotides at the very beginning of 5' UTR. *Sph*I was the restriction endonuclease recognition site introduced between the CMV and T7 promoter, indicated by arrowhead. Letters of lowercase type were modification in T7 promoter.

versity) at 1:600 dilution for 2 h at 37 °C. After five times wash, the cells were incubated at 37 °C for 1 h with Alexa Fluor 568-labeled goat anti-mouse IgG (H+L) (Invitrogen). Fluorescence signal was visualized using an inverted Fluorescence microscope (Olympus IX71), as previously described (Lv et al., 2008; Sun et al., 2010). For the detection of viability of the mutant transfectants on BHK-21 cells, the anti-N IFA was repeated at 48 h post infection (hpi), using P0 viral supernatants from BHK-21 cells on the MARC-145 cell monolayer.

2.5. 5' RACE, RT-PCR and nucleotide sequencing

The series of 5'-terminal mutant viruses (P1–P5) were harvested from MARC-145 cells after 48 hpi. Total cellular RNA was extracted using TRIzol® reagent (Invitrogen) and stored at –80 °C. 100 ng of cellular RNA was used for the reverse transcription with 10 pM SR2573, incubated at 42 °C for 30 min and placed on ice according to the instruction of Avian myeloblastosis virus (AMV) reverse transcriptase (TaKaRa, Dalian, China). The reverse transcribed product was purified via QIAgen PCR product purification kit (QIAgen, Hilden, Germany) and the cDNA was eluted in 40 µL of Nuclease-free water. Poly (G)-tailing (TaKaRa) were added to the 3' terminal of purified PRRSV cDNA using a terminal deoxynucleotide transferase (TdT, New England Biolabs), as instructed by the manufacturer, and then eluted into 60 µL ddH₂O and stored at –30 °C for further use. First round PCR was completed as described previously (Yuan et al., 2001) using 2 pM Qc and 10 pM Qo as the forward primers and 10 pM SR1124 as the reverse primer, included 30 cycles of 95 °C denaturation for 30 s, annealing at 58 °C for 30 s, and extension at 72 °C for 1 min. An identical second round of PCR was then performed using 1 µL first round PCR product and Qi and SR683 as the primer pair. Amplification protocol consisted of 30 cycles of 95 °C denaturation (30 s), 55 °C annealing (30 s), and 72 °C extension (40 s), followed by one round of 10 min incubation at 72 °C. After electrophoresis in 1% agarose gel, the PCR products were purified by QIAquick gel-purification kit (QIAgen), and then were used directly as templates for subcloning and nucleotide sequencing, which conducted with the DNASTAR program (Lasergene Package). Besides, vAPRRSM4, vAPRRSM12 and vAPRRSM16 (P1–P5) were verified by full-length sequencing. The primers for full-length sequencing are available upon request.

2.6. Viral plaque assay

Virus stocks of P1 were chosen for infecting MARC-145 cells monolayer of 6-well plates at 0.01 multiplicity of infection (MOI), after 1 h incubation at 37 °C under 5% CO₂. The inocula were discarded and cells were washed with PBS thrice, and the cell monolayers were then overlaid with pre-made MEM, which comprised by 2× MEM (Invitrogen) with 4% FBS and equal amount of 2% low melting agarose (Cambrex, Rockland, ME, USA), then incubated at 37 °C under 5% CO₂. The resulting plaques were stained with crystal violet (5% (wt/vol) in 20% ethanol) at 5 days post infection (dpi) (Sun et al., 2010; Yu et al., 2009; Zheng et al., 2010). Virus passage was conducted by plaque to plaque purification, solidified agarose gel containing a visible plaque was obtained and piped into a tubes, which containing 500 µL EMEM without FBS. After freezing and thawing thrice, centrifugating at 12,000 × g for 10 min, the supernatant was used directly for infecting MARC-145 cells. The next generation of viral plaques were picked and treated as mentioned above (Zheng et al., 2010).

2.7. Viral titers of first cycle and growth kinetics of mutant viruses

All the mutant and WT plasmids were transfected into BHK-21 cells of 12-well plates. The supernatants (P0) were harvested

48 hpt, and the viral titers were evaluated by 50% tissue culture infective dose (TCID₅₀ mL⁻¹) (Pizzi, 1950) on MARC-145 cells. 90% Confluence of MARC-145 cells were grown in 96-well plates. 100 µL supernatants of 10-fold serial dilution by EMEM with 2% FBS, containing stoste, 10⁻¹, 10⁻², 10⁻³, 10⁻⁴, 10⁻⁵ were inoculated in each well. Every dilution repeated four wells. After 5 days of infected, the CPE wells were read out for values analysis. For growth curve analysis, MARC-145 cells were infected with all of the mutant viruses (P1), vAPRRSM2, M4, M6, M8, M10, M12, M14, M16 of P1, and WT at 0.01 MOI. Each experiment was independently repeated for three times. After 1 h of adsorption, the inocula were washed away. MARC-145 cells were infected with related viruses until 0, 12, 24, 36, 48, 60, 72, 84, 96, 108 h, respectively. 200 µL Supernatants were harvested at all time points above and frozen at –80 °C until use. Relevant wells were replenished with 200 µL EMEM with 2% FBS. Viral titration was conducted through quantitation by viral plaque assay on MARC-145 cell monolayers (Sun et al., 2007; Yu et al., 2009).

2.8. Northern blot analysis

Northern Blot was performed according to the NorthernMax kit (Ambion Austin, TX) manufacturer's protocol. MARC-145 cells were infected with mutant viruses, and WT (P1) at 1 MOI. Total intracellular RNAs were isolated from infected cells which collected at 36 hpi using TRIzol® reagent (Invitrogen). The total RNAs were separated on 1% denatured agarose gels using Agarose-LE (Ambion, Austin, TX) as described previously (Sun et al., 2010, 2007; Yuan and Wei, 2008), and blotted onto a nitrocellulose membrane (Ambion, Austin, TX), and probed with an N-specific probe PR3 (listed in Table 1). The hybridization was incubated at 42 °C overnight, followed by washing with low/high-stringency buffer, wash buffer, blocking buffer (Ambion, Austin, TX). The membrane was incubated with the chemiluminescent substrate CDP-STAR (Ambion, Austin, TX). Exposed the blot on film overnight in darkness and obtained the image.

2.9. RNA secondary structure analysis

RNA secondary structures were predicted using the RNAviz software and the energy minimization program of Mfold website server (<http://mfold.rna.albany.edu/?q=mfold/RNA-Folding-Form>) (Zuker, 2003) and the secondary structure drawing and modifying software RNAviz version 2.0 (<http://rnnaviz.sourceforge.net/>) (De Rijk et al., 2003).

3. Results

3.1. Reverse genetic manipulation of the 5' proximal end of PRRSV genome

To identify possible cis-acting regulatory sequence and/or structural signals residing in the 5' genomic end, we set out to conduct reverse genetic manipulation, based on the PRRSV full-length cDNA clone pAPRRS. As shown in Fig. 1, pAPRRS was driven by both the human cytomegalovirus immediately early promoter (CMV) and T7 promoter (T7), with which either “DNA-launched” or “RNA-launched” reverse genetics can be conducted (Yuan and Wei, 2008). In general, the desired mutations were included in the synthetic forward primers (Table 1). A series of mutant full-length cDNA clones with 5'-terminal authentic sequences of 5' UTR deleted were constructed. Upon verified by restriction endonuclease mapping and nucleotide sequencing, these full-length mutant plasmids were named as pAPRRSD1, D3, D4, D5, D6, pAPRRSM1, M2, M3, M4, M5, M6, M7, M8, M9, M10, M11, M12, M13, M14, M15, M16, M17, M18, M19, M20, M21, M22, M23, M44, M68, M99, M190, Mzg3 and Mzg6,

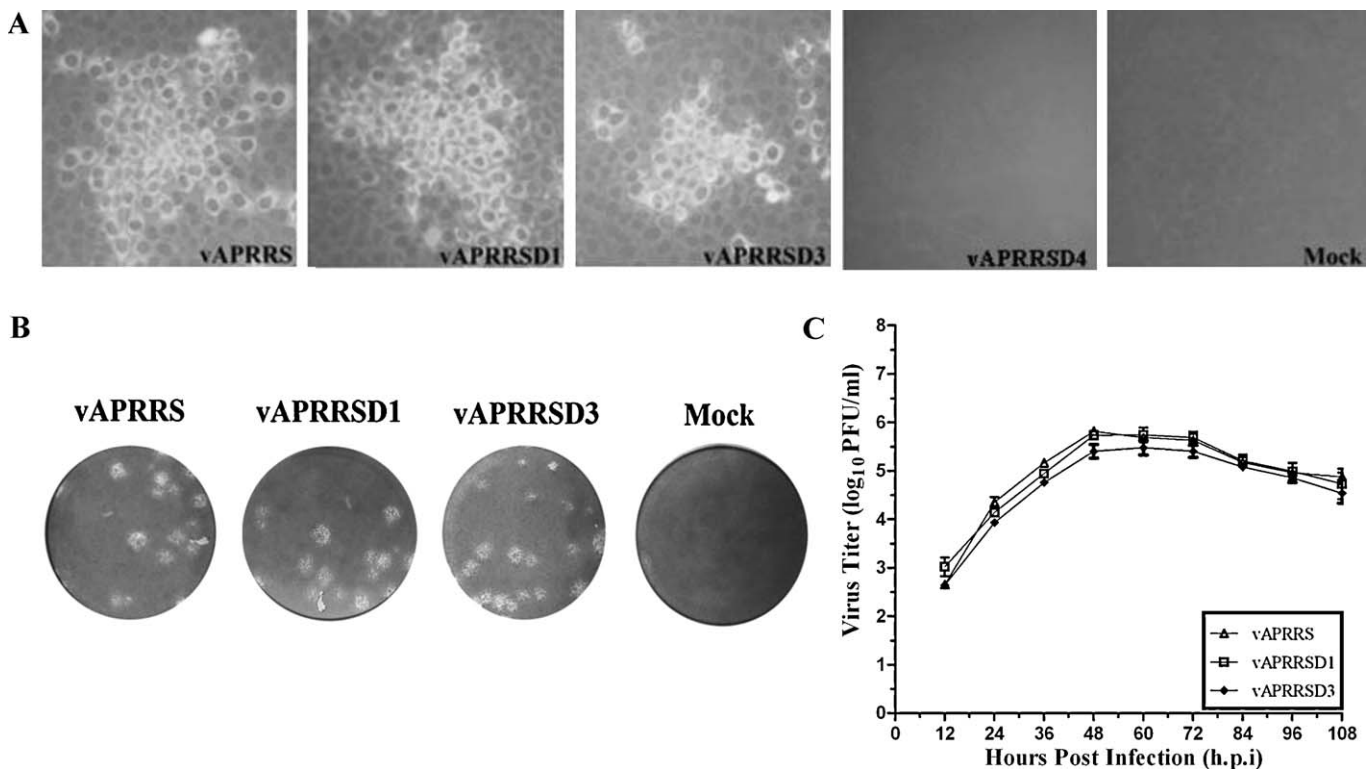


Fig. 2. Nucleocapsid protein expression and virologic properties of the WT and RNA-launched mutant viruses. (A) PRRSV N protein expression of WT and mutants in transfected cells visualized by IFA. At 48 hpi, the cell monolayer was fixed and stained with the N-specific MAb and Alexa Fluor 568 goat anti-mouse IgG (H+L). (B) Viral plaque morphology assay of vAPRRSD1 and D3. P1 viral stocks of 0.01 MOI were inoculated in fresh MARC-145 cells and covered by MEM containing 2% FBS and 1% agarose-LE, and the plaques of the WT and mutant vAPRRSD1, SD3 were visualized at 6 dpi by crystal violet staining. (C) Multi-step growth curve determination. 0.01 MOI of P1 WT and mutant viruses were used for infecting fresh MARC-145 cells, supernatants were harvested at the indicated time points. The virus titers were determined by viral plaque assay and expressed as log₁₀ PFU/mL.

of which the representative plasmids are drawn in Fig. 1. All the mutants were divided into three groups. Mutant cDNA clones of group I were intended to be used as templates for in vitro genomic RNA synthesis, by T7 DNA-dependent RNA polymerases in the RNA-launched form. On the other hand, group II and group III, controlled under CMV promoter, were directly transfected into cells in a form of DNA-launched RGS. Moreover, the T7 promoter was substituted as GC-rich sequences in pAPRRSMzg3 and pAPRRSMzg6. As shown in Fig. 1, the transcription initiation site of CMV promoter was located in the T7 promoter if DNA-launched transfection was used, thus the in vivo synthesized RNA genomes contained 9 extra foreign nucleotides (CAC UAU AGG) immediately before the viral sequence.

3.2. The first three nucleotides at 5' end of PRRSV were nonessential for virus viability

To investigate the role of the PRRSV 5' terminal nucleotides in viral replication, WT, pAPRRSD1, D3, D4, D5, D6 were lineared by Xho I, located immediately after the poly (A) tail, based on which in vitro transcription was performed for preparation of genomic RNAs. Upon transfection into MARC-145 cell monolayers, APRRSD1 and D3 transcripts, similar to APPRS, developed cytopathic effect (CPE) at 6 days post transfection (dpt) and the supernatant was harvested as passage 0 (P0). The mutant transcripts containing four or more nucleotide deletions, i.e., APRRSD4, D5 and D6 failed to develop any CPE, even after prolonged incubation. Moreover, the transfectant supernatants were transferred to fresh MARC-145 cells for three blind passages, no CPE was observed and viral sequence specific RT-PCR detect no PRRSV sequence in both the infected culture supernatants and the total intracellular RNAs (data not shown). These results confirmed previous reports that authentic 5' proximal

sequences were not required for initiation of PRRSV replication (Choi et al., 2006).

PRRSV nucleocapsid (N) protein expression was assessed by indirect immunofluorescence assay (IFA) with monoclonal antibody against N protein at 48 hpt. As shown in Fig. 2A, the expression of N protein was detected in pAPRRSD1, D3, but not D4, of which the defect could be upstream of N translation, e.g., mRNA7 transcription. The growth characteristics of P1 viable mutant viruses, vAPRRSD1 and vAPRRSD3 were compared with WT in MARC-145 cells. While the plaque morphology of the mutant viruses was indistinguishable from that of the parental virus (Fig. 2B), vAPRRSD3 produced slightly lower viral titer than vAPRRSD1 and vAPRRS, especially in the early stage of the multi-step growth curve (Fig. 2C).

To investigate the fate of the engineered mutations, 5' rapid amplification of cDNA end (RACE) and nucleotide sequencing was conducted. Surprisingly, both vAPRRSD1 and vAPRRSD3 restored their terminal end by adding extra yet different nucleotides from the authentic sequence. The direct sequencing results of the RT-PCR products revealed that mutant D1 and D3 contained sequence as "AgaA" or "AguA", of which the sequence in lower case represented that were different from the original authentic sequences (data not shown). Moreover, the acquired sequences were genetically stable even after five passages of purified plaque. In summary, all the results above demonstrated that the 5' proximal three nucleotides were nonessential for viral viability and rescued mutant viruses could acquire some exogenous sequences, which distinct from authentic 5'-end. Although the mutant viruses shared the similar characteristics with their parental virus, it was apparent that the growth kinetic of vAPRRSD3 slightly decreased compared with the other viruses.

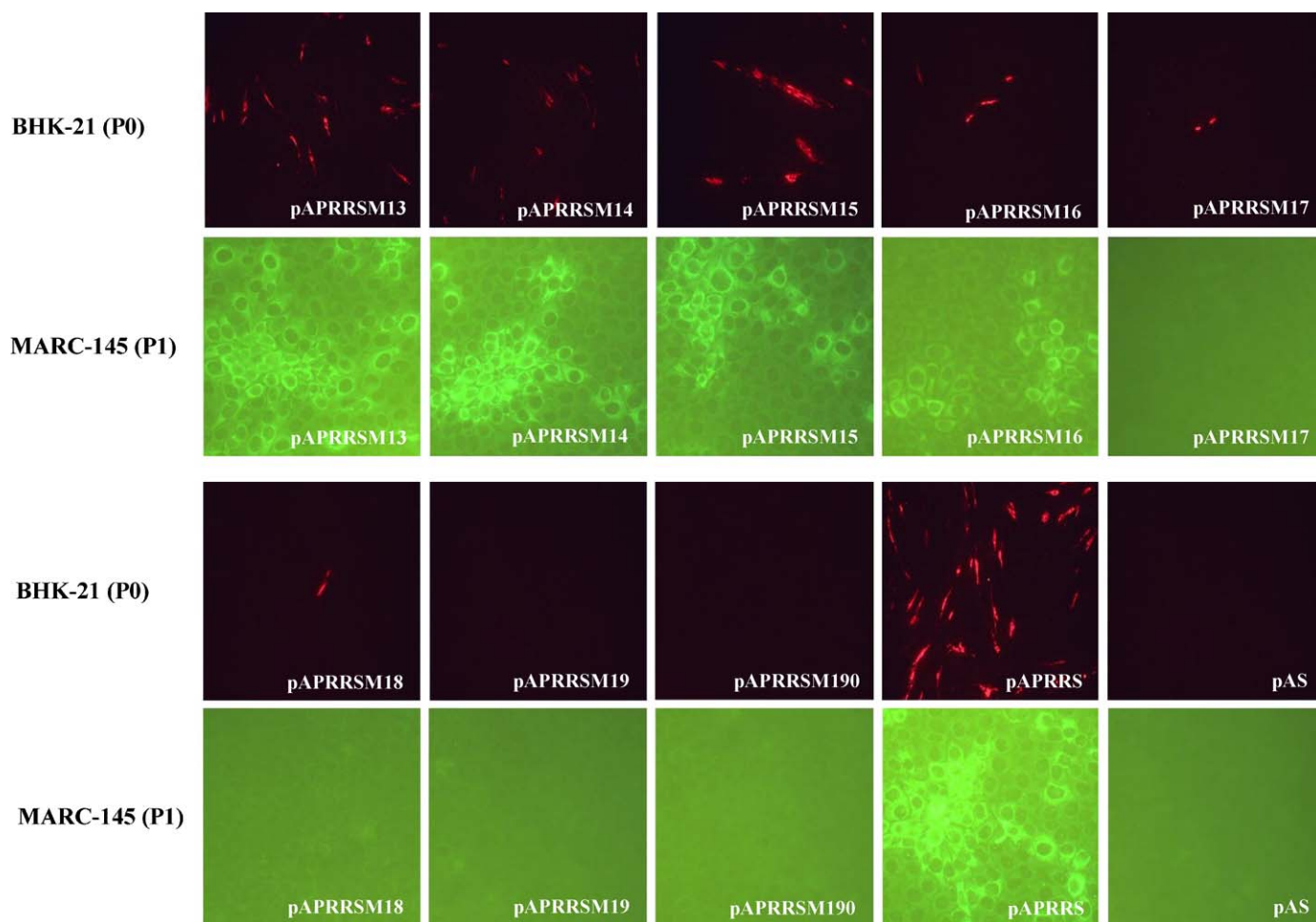


Fig. 3. IFA of the transfected BHK-21 cells by PRRSV 5' UTR serial deletion mutants. WT, serial deletion mutants and negative control were transfected into fresh BHK-21 cells by LTX reagent (Invitrogen). The supernatants were harvested at 24 hpt as P0. Undiluted P0 supernatants were used for incubating fresh MARC-145 cells, and the supernatants were harvested at 48 hpi. The cell monolayer of the transfected BHK-21 and infected MARC-145 cells was fixed and stained by anti-N antibody and Alexa Fluor 568 goat anti-mouse IgG (H+L) at 24 hpt or 48 hpi. The IFA pattern was shown for the WT and mutant viruses, labeled by pAPRRS, pAPRRSM13–19, SM190, and the pAS negative control. Note: Only representatives were shown, due to the space limit.

3.3. The 5' terminal 16 nucleotides could be altered without losing viral infectivity

We next investigated if the different foreign sequences could functionally replace the authentic 5'-terminal nucleotide sequences. To this end, we utilized the DNA-launched system. Because that the transcription initiation sites by CMV promoter were located in the T7 promoter, therefore the *in vivo* synthetic genomic RNAs would contain the 9 extra nucleotide sequence at the 3' end of T7 promoter, immediately following the canonical CMV transcription start site according to the USA patent 5,168,062 by Mark F. Stinski. The mutant plasmids were transfected into BHK-21 cells. At 24 hpt, IFA was performed for detecting PRRSV N protein expression as described above. Fig. 3A reveals that N protein was detected with deletions that was up to 18 nucleotides in pAPRRSM18 (IFA results for pAPRRSM1 through M12 were not shown, due to page limit). Mutant plasmids containing more than 18 nucleotides deletion, as well as the nonreplicative control pAS, were negative even after prolonged incubation for 7 dpt, and three subsequent blind passages. Moreover, the expression level of N protein was invertedly correlated to the number of the nucleotides deleted, and only a few secluded spots were found in pAPRRSM17 and M18 transfected wells (Fig. 3). In addition, IFA with anti-Nsp2

antibody results revealed that all mutants including pAPRRSM190 containing no leader sequence at all, expressed Nsp2 protein, which was translated from the CMV-driven genomic RNAs (data not shown). Again, the expression level were different, with mutants containing more than 16 nucleotide deletion only displayed sparse positive cells, implying that the first 16 nucleotides could have a role for virus replication.

To test the viability of the mutant transfectants, the supernatant of all N protein positive mutants (P0) were harvested for further passage in fresh MARC-145 cells. Anti-N IFA was repeated at 48 hpi. The result showed that all mutants except vAPRRSM17 and vAPRRSM18 expressed PRRSV N protein, indicating that the transfectant vAPRRSM1–16 were infectious (Fig. 3). To test the infectivity of deletion mutants, the supernatant of the transfected BHK-21 cells at 48 hpt was harvested for titration in MARC-145 cells. The viral titers were gradually decreasing along with the deletion number of the 5' proximal nucleotides. The viral titers of mutant vAPRRSM15 and M16 were the two lowest among them, was $1 \times 10^{0.5}$ TCID₅₀ mL⁻¹ and $1 \times 10^{0.33}$ TCID₅₀ mL⁻¹, ~1500-fold and ~2200-fold lower than $1 \times 10^{3.67}$ TCID₅₀ mL⁻¹ of WT, respectively (Fig. 4A). The supernatants were harvested at 5 dpi, and designated as passage 1 (P1). The representative P1 viruses were inoculated into MARC-145 cells for the assessment of growth

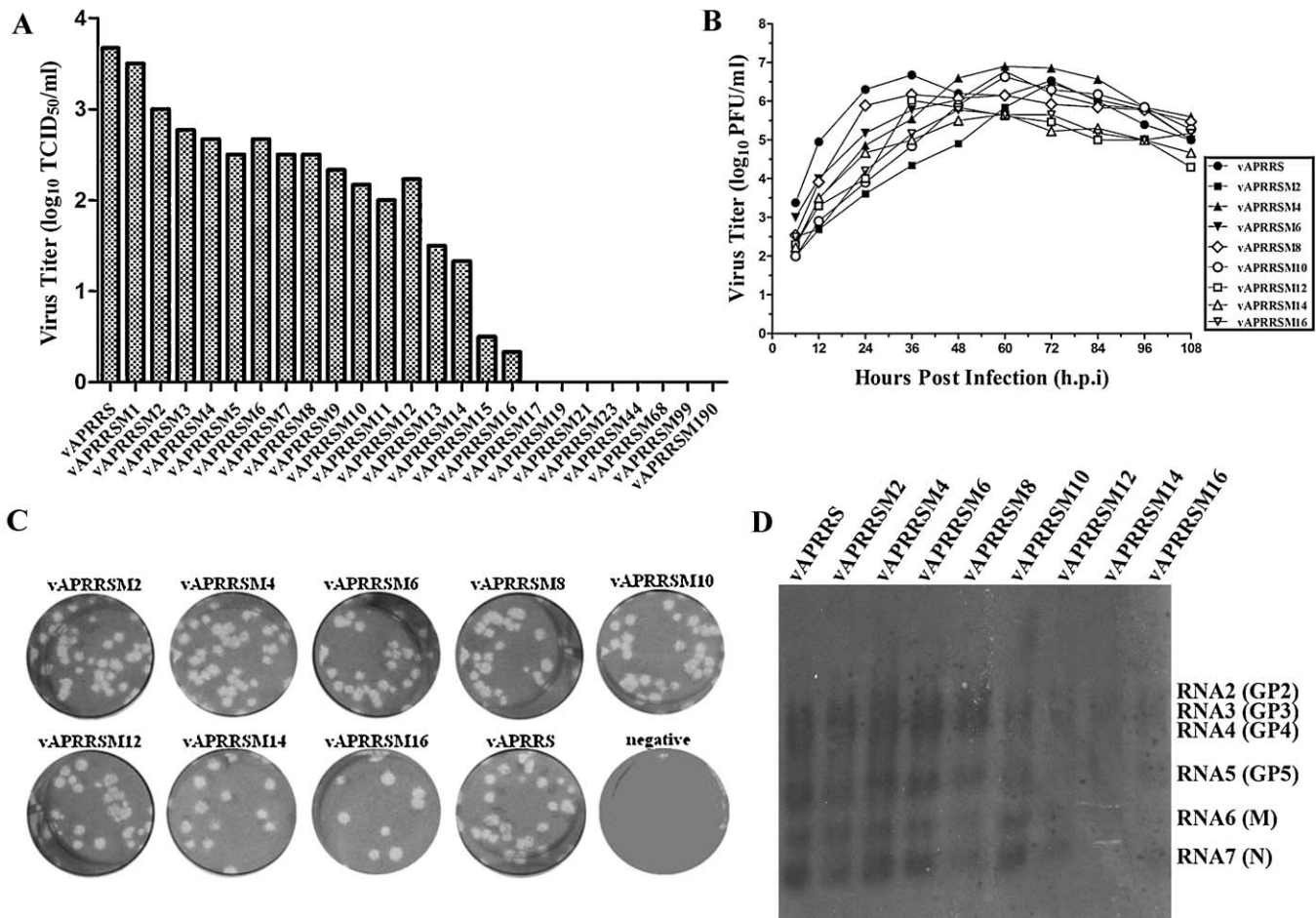


Fig. 4. Phenotypic characterization of rescued DNA-launched mutant viruses. (A) Growth phenotypic properties of DNA-launched mutants were analysed by viral titer determination. The transfection supernatants were harvested from BHK-21 cells at 48 hpt, and then directly used for TCID₅₀ measurement. Viral titers were shown for the WT and mutants, labeled by vAPRRS, vAPRRSM1–17, SM19, SM21, SM23, SM44, SM68, SM99 and SM190. (B) Plaque morphology of mutant viruses and WT. P1 viral stocks of 0.01 MOI were chosen for infecting fresh MARC-145 cells and the plaques were stained with crystal violet 6 dpi. (C) Growth characteristics of WT and mutant viruses were performed by multi-step growth curve. MARC-145 cells were infected by mutant and WT (P1) of 0.01 MOI. Viral progeny was harvested at indicated time points, followed by viral titration by plaque assay on MARC-145 cells, and expressed as log₁₀ PFU/mL. (D) Viral RNA transcription process was investigated by Northern blot. Fresh MARC-145 cells were infected by vAPRRSM2, M4, M6, M8, M10, M12, M14 and M16 (P1) at an MOI of 1. Intracellular RNAs were extracted at 36 hpi. The RNAs were separated on denaturing 1% agarose gels, blotted onto a nitrocellulose membrane (Ambion), and probed with type II 3' UTR-specific probe PR3 and sg mRNA 2–7 were labeled.

properties. Compared with the parental virus, vAPRRSM2, M4, M6, M8, M10, M12, M14 and M16 displayed the similar viral plaque morphology (Fig. 4B). Multi-step growth curves revealed that the virus yield was decreased for all of the deletion mutants, especially in the earlier phase. However, the peak titer at 72 hpi difference became smaller than that in the earlier phase (Fig. 4C), suggesting that there might be restoration of virus infectivity during such multiple cycles of infection compared with the viral titer of the first cycle, as shown in Fig. 4A. Taken together, these results demonstrated that alternation of the first 16 nucleotides were not lethal for virus infectivity, albeit the virus yield was generally affected to some extent.

To analyse the viral RNA profiles, total RNAs were isolated at the 36 hpi from MARC-145 cells infected by the P1 mutant viruses at MOI of 1. The separated RNAs on formaldehyde-denatured agarose gel were blotted with the DIG-labeled PR3 probe that is complementary to the 3' UTR sequences of type II PRRSV (Table 1). The Northern blot results revealed that the sg mRNAs of mutants could be recognized by the specific probe and the sg mRNA7 was the most abundant RNA in the virus transcription process. These results demonstrated that the transcription patterns in mutant virus were not dramatically changed despite that up to 16 nucleotides at the 5' terminus were altered. But the sg mRNA abundance was grad-

ually decreasing along with the deletion number of nucleotides in PRRSV 5' end (Fig. 4D). This result was also consistent with that of first cycle viral titration (Fig. 4A).

3.4. The altered 5' proximal regions were repaired by exogenous AU-rich sequences

To further investigate the roles of the deleted or substituted 5' proximal sequence, 5' RACE, molecular cloning and nucleotide sequencing were performed with P1 of the representative mutant viruses. The nucleotide sequences at the very beginning of 5' terminal regions of all rescued mutant viruses were determined. We found that the rescued viruses contained foreign sequences at their authentic sequences deletion region, as summarized in Fig. 5A. In this DNA-launched system, the in vivo synthetic RNAs contained 9 extra nucleotides from the T7 promoter. Interestingly, the rescued virus vAPRRS (P0) was identical to the authentic genomic RNA (¹AUGACGUUAGGUGUUGGCUC²¹), implying that the exogenous nonviral sequences did not affect virus replication and were then eliminated during virus replication process.

We further compared the altered sequences introduced into the in vivo synthetic RNAs, represented by the plasmid name in

		1	10	20	30	40				
A	pAPRRS	taatac gactcactataggATGACGTATAGGTGTTGGCTCTATGCCTTGACATTTGTATT					No.of clones			
	vAPRRS	ATGACGTATAGGTGTTGGCTCTATGCCTTGACATTTGTATT						10/10		
	pAPRRSM10	cactatagg -----	GGTGTGGCTCTATGCCTTGACATTTGTATT							
	vAPRRSM10S1		f a c t a t a g g	GTTGGCTCTATGCCTTGACATTTGTATT			7/9			
	vAPRRSM10S2		a c t a t a g g	GGTGTGGCTCTATGCCTTGACATTTGTATT			2/9			
	pAPRRSM12	cactatagg -----	TGTTGGCTCTATGCCTTGACATTTGTATT							
	vAPRRSM12S1		a t t a t a t a t a g g	TGTGGCTCTATGCCTTGACATTTGTATT			2/8			
	vAPRRSM12S2		a c t a t a t a t a g g	TGTGGCTCTATGCCTTGACATTTGTATT			2/8			
	vAPRRSM12S3		a t a t a t a t a t a g g	TGTGGCTCTATGCCTTGACATTTGTATT			4/8			
	pAPRRSM14	cactatagg -----	TTGGCTCTATGCCTTGACATTTGTATT							
	vAPRRSM14S1		t a t a t a g g	TGTGGCTCTATGCCTTGACATTTGTATT			6/9			
	vAPRRSM14S2		t a t a t a t a g g	TGTGGCTCTATGCCTTGACATTTGTATT			3/9			
	pAPRRSM16	cactatagg -----	GGCTCTATGCCTTGACATTTGTATT							
	vAPRRSM16S1		t a c t a t a g g	GGCTCTATGCCTTGACATTTGTATT			4/10			
	vAPRRSM16S2		a t t a t a t a g g	GGCTCTATGCCTTGACATTTGTATT			6/10			
	pAPRRSMzg3	gcg tccc---	ACGTATAGGTGTTGGCTCTATGCCTTGACATTTGTATT							
	vAPRRSMzg3S1		a t t a t a	ACGTATAGGTGTTGGCTCTATGCCTTGACATTTGTATT			1/9			
	vAPRRSMzg3S2		a t a t a t a	ACGTATAGGTGTTGGCTCTATGCCTTGACATTTGTATT			8/9			
	pAPRRSMzg6	gcg tccc-----	TATAGGTGTTGGCTCTATGCCTTGACATTTGTATT							
	vAPRRSMzg6S1		a t a t a t a t a	TATAGGTGTTGGCTCTATGCCTTGACATTTGTATT			3/8			
vAPRRSMzg6S2		a t a t a t a	TATAGGTGTTGGCTCTATGCCTTGACATTTGTATT			5/8				
B	pAPRRS	taatac gactcactataggATGACGTATAGGTGTTGGCTCTATGCCTTGACATTTGTATT					Passage	No.of clones		
	pAPRRSM12	cactatagg -----	TGTTGGCTCTATGCCTTGACATTTGTATT							
	vAPRRSM12S2		a c t a t a t a t a g g	TGTGGCTCTATGCCTTGACATTTGTATT			P1	4/4		
			a c t a t a t a t a g g	TGTGGCTCTATGCCTTGACATTTGTATT			P2	4/4		
			a c t a t a t a t a g g	TGTGGCTCTATGCCTTGACATTTGTATT			P3	4/4		
			a c t a t a t a t a g g	TGTGGCTCTATGCCTTGACATTTGTATT			P4	4/4		
			a c t a t a t a t a g g	TGTGGCTCTATGCCTTGACATTTGTATT			P5	4/4		
	pAPRRSM14	cactatagg -----	TTGGCTCTATGCCTTGACATTTGTATT							
	vAPRRSM14S1		t a t a t a g g	TGTGGCTCTATGCCTTGACATTTGTATT			P1	4/4		
			t a t a t a g g	TGTGGCTCTATGCCTTGACATTTGTATT			P2	4/4		
			t a t a t a g g	TGTGGCTCTATGCCTTGACATTTGTATT			P3	4/4		
			t a t a t a g g	TGTGGCTCTATGCCTTGACATTTGTATT			P4	4/4		
			t a t a t a g g	TGTGGCTCTATGCCTTGACATTTGTATT			P5	4/4		
	pAPRRSMzg3	gcg tccc---	ACGTATAGGTGTTGGCTCTATGCCTTGACATTTGTATT							
	vAPRRSMzg3S2		a t a t a t a	ACGTATAGGTGTTGGCTCTATGCCTTGACATTTGTATT			P1	4/4		
			a t a t a t a	ACGTATAGGTGTTGGCTCTATGCCTTGACATTTGTATT			P2	4/4		
			a t a t a t a	ACGTATAGGTGTTGGCTCTATGCCTTGACATTTGTATT			P3	4/4		
			a t a t a t a	ACGTATAGGTGTTGGCTCTATGCCTTGACATTTGTATT			P4	4/4		
			a t a t a t a	ACGTATAGGTGTTGGCTCTATGCCTTGACATTTGTATT			P5	4/4		

Fig. 5. The cDNA sequence alignment for genetically stable, exogenous AU-rich sequences located in the 5' proximal regions of mutant viruses. (A) Schematic representation of the filling-in cDNA sequences at the utmost 5' end of the mutant viral genome. "cactatagg" for in vitro synthetic RNA APRRSM10, M12, 14, 16 was denoted in boldface and lowercase type, while the sequence of APRRSMzg3 and Mzg6 was "gcg tccc". T7 promoter sequence "taatac gactcactatagg" was also shown. The different kinds of exogenous AU-rich sequences obtained by 5' RACE were denoted follows. The tag "S1", "S2" and "S3" indicated restorations using nonviral foreign sequences. Hyphens indicated the deleted nucleotide sequences. The numbers of clones for nucleotide sequencing were indicated in right lane. (B) The sequence stability was detected via 5' RACE, using vAPRRM12S2, vAPRRSM14S1 and vAPRRSMzg3S2 as representatives. The 5' terminal sequences of mutant virus for every passage (P1–P5) were indicated in boldface and lowercase type and were stable among in vitro cell culture passage.

Fig. 5A, with those recovered from transfectant viruses. The 5' terminal sequence of each viable virus was determined by sequencing 8 to 10 clones of the 5' RACE products, and the sequencing results revealed that the revertant viruses all contained diversified AU-rich sequences, which is variable in length and different from either the template DNA or the authentic sequence in PRRSV 5' UTR (Data not shown). As shown in Fig. 5A, the cDNA sequences of in vivo synthetic RNA from pAPRRSM10 contained deletion of the first 10 nts, 9 of which would be filled-in by the nonviral sequence derived from T7 promoter. However, all nine clones displayed sequences "actatagg" from the nonviral T7 promoter sequence tem-

plate, which were different from and one nucleotide short than the authentic 5' UTR. Moreover, 7 out of the 9 clones also contained a non-T7 templated "t" at the 5' end. In pAPRRSM12, M14, and M16, the in vivo synthetic RNAs were 3–7 nucleotides short than the authentic PRRSV 5' UTR after addition of the nonviral T7 sequence (Fig. 5A). Nucleotide sequence determination results revealed that all of these recovered viruses contained AU-rich sequences, with unknown origin except the T7-templated "tatagg" immediately before the viral sequence.

To investigate the origin of the repaired nucleotides, we changed the T7 promoter sequences such that the 5' end of the synthetic

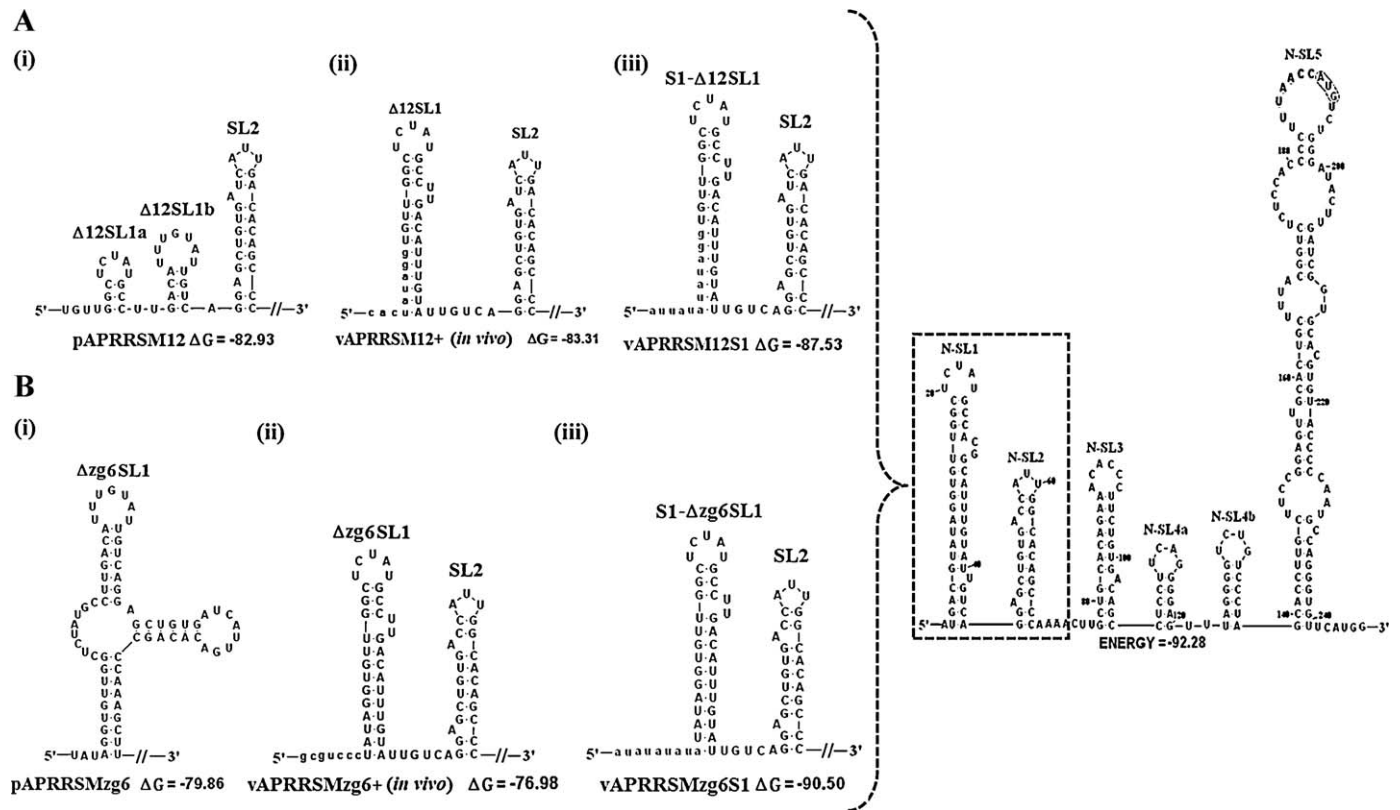


Fig. 6. Secondary structure models of the pAPRRSM12, pAPRRSMz6 and their reverted viruses. 5' terminal sequences corresponding to nt 246 were predicted by Mfold, and modified by RNAviz. (A) The secondary structure of entire 5' UTR and part of ORF1a of pAPRRS. stem-loop (SL) 1 and SL2 of pAPRRSM12, *in vivo* synthetic RNA, vAPRRSM12+ and a representative restoration, vAPRRSM12S1 in their 5' UTR. Broken-line box denoted SL1 and SL2 in pAPRRS. "Δ" denoted nucleotide deletions. Nonviral novel sequences were shown in lowercase type. "/" indicated elsewhere sequences of genomic RNA. The tag "S1" and "S2" indicated restorations using nonviral foreign sequences, which shown in lowercase type. (B) The secondary structures of entire 5' UTR of pAPRRS, SL1 and SL2 of pAPRRSMz6, vAPRRSMz6+ and vAPRRSMz6S1 in their 5' UTR were also shown.

RNAs would be GC-rich. Upon transfection, the rescued viruses of vAPRRSMz6 and vAPRRSMz6g all contained AU-rich sequences, indicating that the repaired 5' end was template-independent (Fig. 5). In summary, we found that not only "a" and "u" could be utilized by the revertant viruses for end repair, but also "g" and "c". It nonetheless appeared that AU-rich sequences were preferred. In addition, nucleotide length of some restoration sequences was shorter than that of original deleted sequence, while the others were longer.

3.5. The end-repaired mutant viruses were genetically stable

To further assess the genetic stability during serial passages via plaque purification, the mutant viruses were infected in MARC-145 cells at 0.01 MOI. All the culture supernatants were harvested as viral stocks of P1 to P5. 5' RACE was performed to detect the 5' terminal restoration sequences of every passage. Fig. 5B shows vAPRRSM12, M14, Mz6g restoration revertant vAPRRSM12S2, M14S1, Mz6gS2. The original mutation sites were stably maintained at least for 5 passages. No matter the restoration sequence was shorter or longer than that of original deleted sequence. They all retained the great similarity with each other without any mutation in the flanking region. Full-length genomic sequence determination was also conducted for vAPRRSM4, M12 and M16. The direct sequencing for the RT-PCR products revealed no conspicuous genomic sequence alteration in the virus (P1–P5) population (data not show). These results demonstrated that once restored, the obtained 5' terminal sequences of each mutant viruses (P1–P5) were stable, and the mutant sequences existed in rescued

virus genome and stable among *in vitro* cell culture passage (data not shown).

3.6. Structural rather than primary sequence elements regulate PRRSV replication

It is generally believed that structural elements play important roles in the control of positive-strand RNA viruses (Liu et al., 2009). We next assessed the possible effects of the sequence truncations and alterations to the putative structures of the PRRSV 5' proximal sequences. The predicted secondary structure of 5' terminal 246 nucleotides of APRRSV was shown in Fig. 6. A total of 6 stem-loops were predicted and verified by multiple Algorithms. The overall secondary structure was dramatically changed when the first 12 nucleotides "1ATGACGTATAGG12" were deleted in pAPRRSM12 (Fig. 6Ai). In particular, the original stem-loop 1 (SL1) was replaced with two minor stem-loops. However, the filling-in by the T7 promoter sequence restored the SL1-like structure, though the sequence is different (Fig. 6Aii). Surprisingly, all of the sequences in the recovered viable viruses were found to form a SL1-like structure, as represented by that of vAPRRSM12S1 (Fig. 6Aiii). We then analysed the nucleotide deletion and substitution in pAPRRSMz6. Pure deletion of the first 6 nucleotides would disrupt both SL-1 and SL-2 (Fig. 6Bi). However, filling-in by T7 promoter and an artificial GC-rich sequence restored both stem-loops (Fig. 6Bii). Again, all recovered viruses displayed the similar structures, though with different sequence (Fig. 6Biii). Furthermore, we investigated the failure of vAPRRSM17 to initiate virus production, and found that the filling-in by T7 sequences after

deletion of the first 17 nucleotides was not enough to restore the SL1 structure. Overall, we concluded that the SL1, and probably SL2, structure rather than the primary sequence is important for viral infectivity.

4. Discussion

Like other Arteriviruses, PRRSV 5' UTR and 3' UTR are believed to carry a variety of cis-acting elements that regulate the discrete steps of viral RNA synthesis. For example, The leader-TRS hairpin (LTH) structure has been shown to play a central role in EAV subgenomic mRNA synthesis (Pasternak et al., 2001; Van Den Born et al., 2004). But the related experimental evidences have been lacking. By reverse genetic manipulation, we provided the first line of genetic evidences supporting that the SL1 structure of PRRSV 5' UTR play important role for virus viability.

Reverse Genetic System (RGS) has been a powerful tool to investigate the molecular biology of RNA viruses. The first RNA-launched PRRSV RGS was performed for the type 1 Lelystad strain (Meulenberg et al., 1998) by assembling its full-length cDNA under the control of the T7 promoter in the low-copy-number plasmid pOK12. Identical strategies were also previously used in the construction of an infectious cDNA for the North American prototypic VR-2332 strain (Nielsen et al., 2003). In this study, we utilized an infectious cDNA clone pAPRRS that are dually controlled by CMV and T7 promoter (Yuan and Wei, 2008), which offered us more flexibilities for investigating the roles of 5' UTR in the forms of both in vitro and in vivo synthetic genomic RNAs. As the results, we found that the first 16 nucleotides in the PRRSV 5' UTR could be altered without lethal effect to virus infectivity, which is 9 nt longer than that previously reported by Choi et al. (2006). Intriguingly, only 3 nts could be deleted without loss of the viral viability in our RNA-launched system, despite three independent transfections were conducted, and the 4 nt deletion was always lethal for virus recovery. The difference between our observation and that by Choi et al. (2006) may be explained by the genetic diversity between the APRRS and PL97, as only 93.4% identity exist, and 96.3% of 5' UTR. It may be possible that the long-range RNA–RNA interaction and/or the global genomic high-ordered structure were adversely affected by deletion of more nucleotides in APRRS. Alternatively, we found that the SL1 structure was disrupted in the pAPRRSD4, which may be one of the reasons for this lethal mutation.

A great many of plus-strand RNA viruses have been proved that their 5' UTR contains a wide variety of cis-acting RNA elements that are crucial for virus replication (Alvarez et al., 2005; Liu et al., 2009; Van Den Born et al., 2004). Besides acting as RNA signals, high-ordered RNA structure has been confirmed to protect viral RNAs from degradation by exonucleases (Gallie, 1998), and stabilize the genomic RNA (Barton et al., 2001). In our DNA-launched study here, we found that the infectivity of the mutants was directly related to the presence of the SL1, and the lack of which by insufficient substitution, e.g., pAPRRSM17, would render the failure of virus recovery. In fact, both SL1 and SL2 were disrupted in this 17 nt deletion mutant. The viral titration for the first cycle and multiple cycles of mutant viruses were conducted in this study. The viral titers were gradually decreasing along with the deletion number of the 5' proximal nucleotides. But multi-step growth curve revealed that the peak titer of mutant viruses at 72 hpi difference was small, as shown in Fig. 4A and C. According to the exogenous AU-rich sequence detection and secondary structure prediction, it could be deduced that virus viability restoration occurred in viral SL1 structure restoration and stability. The fact that the first 16 nts could be altered without loss of the virus infectivity led us to conclude that the structural RNA, at least SL1, rather than the primary sequence at the PRRSV 5' UTR was crucial for virus replication. Moreover,

all viable viruses acquired nucleotide sequences that invariably restored the SL1 structure, as represented in Fig. 6.

It is generally believed that authentic 5' genomic end was important for RNA virus replication, as well documented in picornaviruses such as poliovirus (Herold and Andino, 2000, 2001), coxsackievirus (Klump et al., 1990). Studies on several plus-strand viruses showed that the nonauthentic nucleotides would be removed during virus replication (Duke and Palmenberg, 1989; Herold and Andino, 2000). In DNA-launched system described here, the in vivo synthetic RNA of pAPRRS contained 9 nt nonauthentic sequences in between the transcription initiate site and the 5' proximal genomic end of PRRSV. However, all the recovered transfectant vAPRRS contained the exact original 5' genomic end of the parental virus. On the other hand, the rescued viruses from the mutants with longer sequence alteration all contained exogenous largely AU-rich sequences, of which the vAPRRSM14S1 was 6 nt shorter than the authentic sequence.

The restoration sequences of the mutant viruses shared great identity with part of T7 promoter sequence behind the CMV transcription initiation site, and were largely AU-rich. To differentiate if the repaired 5' end is template-dependent, we modified the T7 sequence as GC-rich immediately behind the CMV transcription initiation site (Fig. 1, group III). Surprisingly, both rescued viruses, vAPRRSMzg3 and vAPRRSMzg6, were again repaired with AU-rich, indicating that viral genomic end repair is template-independent. At this stage, it was difficult to explain the origin of these novel 5' foreign sequences and the molecular mechanism of their addition at the very beginning of the viral genome. It is likely that they are acquired from cellular RNAs via a process of RNA recombination involving template switching during either negative- or positive-sense RNA synthesis, as has been described for pestivirus (Meulenberg et al., 1993) and poliovirus (Kirkegaard and Baltimore, 1986). Alternatively, the nucleotides were randomly added to the genomic end during RNA synthesis, and the AU-rich sequence containing viruses were selected for their overall better fitness. The selective pressure could come from the sequence requirement for local or long-range RNA–RNA and/or RNA–protein interactions. For instance, the viral RdRp binding site at the 5' end of the Dengue virus genome facilitates template recognition at the 3' end of the genome via long-range RNA–RNA interactions (Filomatori et al., 2007). In addition, the overall high-ordered structures of the 5' UTR or the genomic RNA possibly play a role in the end-repair process, which is supported by our finding that the SL1 is invariably maintained for virus recovery.

The 5' UTR of plus-strand RNA viruses has also documented for multiple functions that regulate the viral life cycles, including genomic RNA translation, replication, subgenomic mRNA (if any) transcription, progeny genome encapsidation (Andino et al., 1990; Choi et al., 2006; Frolov et al., 1998; Herold and Andino, 2001; Liu et al., 2007, 2009; Suzuki et al., 2008; Van Den Born et al., 2004, 2005). In this study, we found that all in vitro and in vivo synthetic genomic RNAs including pAPRRSM190 in which all 5' UTR sequence was deleted were positive for Nsp2 protein expression by IFA (data not shown), demonstrating that the PRRSV 5' UTR has little effect on genomic RNA translation. These results confirmed the finding by the Snijder group showing that none of the EAV 5' UTR sequence or structure played any role in regulating viral RNA translation (Van Den Born et al., 2005). This is not unexpectedly because that nidoviral mRNA translation adopt a leaky-scanning model, while there was probably internal ribosomal entry site (IRES) as those in 5' UTR of a variety of positive-strand RNA viruses (Rijnbrand et al., 1997). However, our IFA results showed that the N protein was not expressed in transfected cells by deletion of the first 19 or more nucleotides, which could be a result of the lack of mRNA7. In addition, our preliminary analyses suggested that the nonviable mutants contained no minus- and probably plus-strand genomic

RNAs. Van Den Born et al. (2005) reported that nt 1–135 in the EAV 5' UTR had little role in subgenomic mRNA synthesis. Therefore, we think that the PRRSV 5' UTR SL1 structure could be an element controlling genomic RNA synthesis.

Taken together, this study demonstrated that (1) the first 3 nucleotides of PRRSV 5' UTR were dispensable for virus viability, though the 5' end of the recovered virus was repaired with different, (2) PRRSV tolerated the first 16 nucleotide sequence alteration of the 5' UTR without losing virus viability, (3) the revertant viruses contained a range of non-templated and unknown origin exogenous nucleotides in the repaired 5' end, and (4) the 5' proximal SL1 structure was invariably required for virus infectivity. We conclude that the SL1 structure rather than its primary sequence is crucial for PRRSV replication.

Acknowledgements

This study was partially supported by the Natural Sciences Foundation of China (30972204 and 30901078) and the EU Frame 7 Program Project (245141) to Shishan Yuan. We thank Dr. Ying Fang at South Dakota State University for generously providing the monoclonal antibody against PRRSV N protein.

References

- Alvarez, D.E., Lodeiro, M.F., Luduena, S.J., Pietrasanta, L.I., Gamarnik, A.V., 2005. Long-range RNA-RNA interactions circularize the dengue virus genome. *J. Virol.* 79 (11), 6631–6643.
- Andino, R., Rieckhof, G.E., Baltimore, D., 1990. A functional ribonucleoprotein complex forms around the 5' end of poliovirus RNA. *Cell* 63 (2), 369–380.
- Barton, D.J., O'Donnell, B.J., Flanagan, J.B., 2001. 5' cloverleaf in poliovirus RNA is a cis-acting replication element required for negative-strand synthesis. *EMBO J.* 20 (6), 1439–1448.
- Boyer, J.C., Haenni, A.L., 1994. Infectious transcripts and cDNA clones of RNA viruses. *Virology* 198 (2), 415–426.
- Cavanagh, D., 1997. Nidovirales: a new order comprising Coronaviridae and Arteriviridae. *Arch. Virol.* 142 (3), 629–633.
- Choi, Y.J., Yun, S.I., Kang, S.Y., Lee, Y.M., 2006. Identification of 5' and 3' cis-acting elements of the porcine reproductive and respiratory syndrome virus: acquisition of novel 5' AU-rich sequences restored replication of a 5'-proximal 7-nucleotide deletion mutant. *J. Virol.* 80 (2), 723–736.
- De Rijk, P., Wuyts, J., De Wachter, R., 2003. RnaViz 2: an improved representation of RNA secondary structure. *Bioinformatics* 19 (2), 299–300.
- den Boon, J.A., Snijder, E.J., Chirnside, E.D., de Vries, A.A., Horzinek, M.C., Spaan, W.J., 1991. Equine arteritis virus is not a togavirus but belongs to the coronaviruslike superfamily. *J. Virol.* 65 (6), 2910–2920.
- Drosten, C., Gunther, S., Preiser, W., van der Werf, S., Brodt, H.R., Becker, S., Rabenau, H., Panning, M., Kolesnikova, L., Fouchier, R.A., Berger, A., Burguiera, A.M., Cinatl, J., Eickmann, M., Escirou, N., Grywna, K., Kramme, S., Manuguerra, J.C., Muller, S., Rickerts, V., Stürmer, M., Vieth, S., Klenk, H.D., Osterhaus, A.D., Schmitz, H., Doerr, H.W., 2003. Identification of a novel coronavirus in patients with severe acute respiratory syndrome. *N. Engl. J. Med.* 348 (20), 1967–1976.
- Duke, G.M., Palmenberg, A.C., 1989. Cloning and synthesis of infectious cardiopvirus RNAs containing short, discrete poly(C) tracts. *J. Virol.* 63 (4), 1822–1826.
- Filomatori, C.V., Lodeiro, M.F., Alvarez, D.E., Samsa, M.M., Pietrasanta, L., Gamarnik, A.V., 2006. A 5' RNA element promotes dengue virus RNA synthesis on a circular genome. *Genes Dev.* 20 (16), 2238–2249.
- Filomatori, C.V., Lodeiro, M.F., Alvarez, D.E., Samsa, M.M., Pietrasanta, L., Gamarnik, A.V., 2007. A 5' RNA element promotes dengue virus RNA synthesis on a circular genome. *Genes Dev.* 20, 2238–2249.
- Frolov, I., McBride, M.S., Rice, C.M., 1998. cis-acting RNA elements required for replication of bovine viral diarrhoea virus-hepatitis C virus 5' nontranslated region chimeras. *RNA* 4 (11), 1418–1435.
- Gallie, D.R., 1998. A tale of two termini: a functional interaction between the termini of an mRNA is a prerequisite for efficient translation initiation. *Gene* 216 (1), 1–11.
- Herold, J., Andino, R., 2000. Poliovirus requires a precise 5' end for efficient positive-strand RNA synthesis. *J. Virol.* 74 (14), 6394–6400.
- Herold, J., Andino, R., 2001. Poliovirus RNA replication requires genome circularization through a protein-protein bridge. *Mol. Cell* 7 (3), 581–591.
- Kirkegaard, K., Baltimore, D., 1986. The mechanism of RNA recombination in poliovirus. *Cell* 47 (3), 433–443.
- Klump, W.M., Bergmann, I., Muller, B.C., Ameis, D., Kandolf, R., 1990. Complete nucleotide sequence of infectious Coxsackievirus B3 cDNA: two initial 5' uridine residues are regained during plus-strand RNA synthesis. *J. Virol.* 64 (4), 1573–1583.
- Ksiazek, T.G., Erdman, D., Goldsmith, C.S., Zaki, S.R., Peret, T., Emery, S., Tong, S., Urbani, C., Comer, J.A., Lim, W., Rollin, P.E., Dowell, S.F., Ling, A.E., Humphrey, C.D., Shieh, W.J., Guarner, J., Paddock, C.D., Rota, P., Fields, B., DeRisi, J., Yang, J.Y., Cox, N., Hughes, J.M., LeDuc, J.W., Bellini, W.J., Anderson, L.J., 2003. A novel coronavirus associated with severe acute respiratory syndrome. *N. Engl. J. Med.* 348 (20), 1953–1966.
- Liu, P., Li, L., Millership, J.J., Kang, H., Leibowitz, J.L., Giedroc, D.P., 2007. A U-turn motif-containing stem-loop in the coronavirus 5' untranslated region plays a functional role in replication. *RNA* 13 (5), 763–780.
- Liu, Y., Wimmer, E., Paul, A.V., 2009. Cis-acting RNA elements in human and animal plus-strand RNA viruses. *Biochim. Biophys. Acta* 1789 (9–10), 495–517.
- Lu, J., Gao, F., Wei, Z., Liu, P., Liu, C., Zheng, H., Li, Y., Lin, T., Yuan, S., 2011. A 5'-proximal stem-loop structure of 5' untranslated region of porcine reproductive and respiratory syndrome virus genome is key for virus replication. *Virology* 428, 172.
- Lv, J., Zhang, J., Sun, Z., Liu, W., Yuan, S., 2008. An infectious cDNA clone of a highly pathogenic porcine reproductive and respiratory syndrome virus variant associated with porcine high fever syndrome. *J. Gen. Virol.* 89, 2075–2079 (Pt 9).
- Meulenbergh, J.J., Bos-de Ruijter, J.N., van de Graaf, R., Wensvoort, G., Moormann, R.J., 1998. Infectious transcripts from cloned genome-length cDNA of porcine reproductive and respiratory syndrome virus. *J. Virol.* 72 (1), 380–387.
- Meulenbergh, J.J., Hulst, M.M., de Meijer, E.J., Moonen, P.L., den Besten, A., de Kluyver, E.P., Wensvoort, G., Moormann, R.J., 1993. Lelystad virus, the causative agent of porcine epidemic abortion and respiratory syndrome (PEARS), is related to LDV and EAV. *Virology* 192 (1), 62–72.
- Nielsen, H.S., Liu, G., Nielsen, J., Oleksiewicz, M.B., Botner, A., Storgaard, T., Faaborg, K.S., 2003. Generation of an infectious clone of VR-2332, a highly virulent North American-type isolate of porcine reproductive and respiratory syndrome virus. *J. Virol.* 77 (6), 3702–3711.
- Pasternak, A.O., Spaan, W.J., Snijder, E.J., 2006. Nidovirus transcription: how to make sense. *J. Gen. Virol.* 87, 1403–1421 (Pt 6).
- Pasternak, A.O., van den Born, E., Spaan, W.J., Snijder, E.J., 2001. Sequence requirements for RNA strand transfer during nidovirus discontinuous subgenomic RNA synthesis. *EMBO J.* 20 (24), 7220–7228.
- Peiris, J.S., Lai, S.T., Poon, L.L., Guan, Y., Yam, L.Y., Lim, W., Nicholls, J., Yee, W.K., Yan, W.W., Cheung, M.T., Cheng, V.C., Chan, K.H., Tsang, D.N., Yung, R.W., Ng, T.K., Yuen, K.Y., 2003. Coronavirus as a possible cause of severe acute respiratory syndrome. *Lancet* 361, 1319–1325 (9366).
- Pizzi, M., 1950. Sampling variation of the fifty percent end-point, determined by the Reed-Muench (Behrens) method. *Hum. Biol.* 22 (3), 151–190.
- Rijnbrand, R., van der Straaten, T., van Rijn, P.A., Spaan, W.J., Bredendijk, P.J., 1997. Internal entry of ribosomes is directed by the 5' noncoding region of classical swine fever virus and is dependent on the presence of an RNA pseudoknot upstream of the initiation codon. *J. Virol.* 71 (1), 451–457.
- Sawicki, S.G., Sawicki, D.L., 1995. Coronaviruses use discontinuous extension for synthesis of subgenome-length negative strands. *Adv. Exp. Med. Biol.* 380, 499–506.
- Snijder, E.J., 2001. Arterivirus RNA synthesis dissected nucleotides, membranes, amino acids, and a bit of zinc. *Adv. Exp. Med. Biol.* 494, 241–253.
- Snijder, E.J., Meulenbergh, J.J., 1998. The molecular biology of arteriviruses. *J. Gen. Virol.* 79 (Pt 5), 961–979.
- Sun, Z., Liu, C., Tan, F., Gao, F., Liu, P., Qin, A., Yuan, S., 2010. Identification of dispensable nucleotide sequence in 3' untranslated region of porcine reproductive and respiratory syndrome virus. *Virus Res.* 154 (1–2), 38–47.
- Sun, Z., Wang, J.Y., Zhang, J.W., Qin, A.J., Yuan, S.S., 2007. Identification of porcine reproductive and respiratory syndrome virus regulation sequence in 3'-untranslated region. *Wei Sheng Wu Xue Bao* 47 (5), 774–778.
- Suzuki, R., Fayzulin, R., Frolov, I., Mason, P.W., 2008. Identification of mutated cyclization sequences that permit efficient replication of West Nile virus genomes: use in safer propagation of a novel vaccine candidate. *J. Virol.* 82 (14), 6942–6951.
- Tian, K., Yu, X., Zhao, T., Feng, Y., Cao, Z., Wang, C., Hu, Y., Chen, X., Hu, D., Tian, X., Liu, D., Zhang, S., Deng, X., Ding, Y., Yang, L., Zhang, Y., Xiao, H., Qiao, M., Wang, B., Hou, L., Wang, X., Yang, X., Kang, L., Sun, M., Jin, P., Wang, S., Kitamura, Y., Yan, J., Gao, G.F., 2007. Emergence of fatal PRRSV variants: unparalleled outbreaks of atypical PRRSV in China and molecular dissection of the unique hallmark. *PLoS One* 2 (6), e526.
- Van Den Born, E., Gultyaev, A.P., Snijder, E.J., 2004. Secondary structure and function of the 5'-proximal region of the equine arteritis virus RNA genome. *RNA* 10 (3), 424–437.
- Van Den Born, E., Posthuma, C.C., Gultyaev, A.P., Snijder, E.J., 2005. Discontinuous subgenomic RNA synthesis in arteriviruses is guided by an RNA hairpin structure located in the genomic leader region. *J. Virol.* 79 (10), 6312–6324.
- van Marle, G., Dobbe, J.C., Gultyaev, A.P., Luytjes, W., Spaan, W.J., Snijder, E.J., 1999. Arterivirus discontinuous mRNA transcription is guided by base pairing between sense and antisense transcription-regulating sequences. *Proc. Natl. Acad. Sci. U.S.A.* 96 (21), 12056–12061.
- Verheije, M.H., Kroese, M.V., Rottier, P.J., Meulenbergh, J.J., 2001. Viable porcine arteriviruses with deletions proximal to the 3' end of the genome. *J. Gen. Virol.* 82 (Pt 11), 2607–2614.
- Verheije, M.H., Olsthoorn, R.C., Kroese, M.V., Rottier, P.J., Meulenbergh, J.J., 2002. Kissing interaction between 3' noncoding and coding sequences is essential for porcine arterivirus RNA replication. *J. Virol.* 76 (3), 1521–1526.
- Yu, D., Lv, J., Sun, Z., Zheng, H., Lu, J., Yuan, S., 2009. Reverse genetic manipulation of the overlapping coding regions for structural proteins of the type II porcine reproductive and respiratory syndrome virus. *Virology* 383 (1), 22–31.

- Yuan, S., Mickelson, D., Murtaugh, M.P., Faaborg, K.S., 2001. Complete genome comparison of porcine reproductive and respiratory syndrome virus parental and attenuated strains. *Virus Res.* 79 (1–2), 189–200.
- Yuan, S., Wei, Z., 2008. Construction of infectious cDNA clones of PRRSV: separation of coding regions for nonstructural and structural proteins. *Sci. China C Life Sci.* 51 (3), 271–279.
- Zheng, H., Sun, Z., Zhu, X.Q., Long, J., Lu, J., Lv, J., Yuan, S., 2010. Recombinant PRRSV expressing porcine circovirus sequence reveals novel aspect of transcriptional control of porcine arterivirus. *Virus Res.* 148 (1–2), 8–16.
- Zhou, L., Yang, H., 2010. Porcine reproductive and respiratory syndrome in China. *Virus Res.* 154 (1–2), 31–37.
- Zuker, M., 2003. Mfold web server for nucleic acid folding and hybridization prediction. *Nucleic Acids Res.* 31 (13), 3406–3415.